Optimal SoC Estimation Considering Hysteresis Effect for Effective Battery Management in Shipboard Batteries

J. Preetha Roselyn, *Member, IEEE*, Anirudhh Ravi, *Member, IEEE*, D. Devaraj, *Senior Member, IEEE*, and R. Venkatesan, *Senior Member, IEEE*

***Abstract*— The energy storage is critical in shipboard systems since there is no alternate energy in case of primary energy source failure. Hence, a battery management system (BMS) is necessary to monitor the state of the battery. Since a BMS operates the battery based on its state, an accurate estimation of the state of charge (SoC) is essential. Hysteresis is predominantly present in lead–acid batteries, whose effect is generally not accounted for in existing SoC estimation methods. In this work, the effect of hysteresis on SoC estimation is considered and the differential evolution-based SoC estimation technique is applied to accurately estimate the SoC while minimizing the hysteresis effect. A dynamic charge and discharge dynamic model of a 100-Ah lead–acid battery with ship thruster load is used to study the battery hysteresis. The battery model with the proposed SoC estimation and the BMS algorithm is simulated in MATLAB/SIMULINK 2018A and is tested under different charging and discharging conditions. The proposed model is validated in a real-time testbed comprising of a 62-Ah lead–acid battery connected to a 25 HP thruster of a boat. From the test results, it has been demonstrated that the proposed estimation algorithm reduces the estimation error thereby achieving an accurate SoC.**

***Index Terms*— Battery management systems (BMS), differential evolution (DE), estimation, hysteresis error, shipboard batteries, state of charge (SoC).**

I. Introduction

LEAD-ACID batteries are the most preferred choice for energy storage, especially for backup purposes, since they are economical, reliable, and robust. These batteries must be utilized efficiently to increase their lifespan. To achieve this, a battery management system (BMS) is highly essential. The use of such BMSs will not only increase the battery lifespan but also will reduce the regular replacement costs, time required for manual maintenance and battery management. To achieve efficient battery management, accurate estimation of major battery parameters such as state of charge (SoC) and state of health is necessary [1].

Over the past decade, various SoC estimation methods have been proposed. These methods have focused on improving the SOC estimation accuracy; however, complexity and estimation time are the tradeoffs. The most conventional and simple method of SoC estimation is the open-circuit voltage (OCV) method [2]. This method is as simple as just connecting a multimeter in parallel to the battery terminals in open-circuit mode and dividing the measured voltage by the rated OCV to obtain the battery's SoC. Though it is simple and quite accurate, the voltage has to be measured when the battery is at rest and it requires a long battery resting period. A similar, but relatively quicker, battery voltage-based SoC estimation method is the terminal voltage method [3] where the ratio of measured terminal voltage to the rated voltage is calculated to obtain the SoC. This method faces a problem during the discharging process where the battery voltage suddenly drops at the end of discharge. Another well-known method with better accuracy than the OCV method is the coulomb-counting (CC) or the Ah-counting method where the measured to rated battery capacity ratio is obtained to calculate the SoC [4]. The only issue with this method is that it does not account for the charge or discharge losses and the self-discharge characteristic of the battery, causing the error to accumulate thereby, reducing the SoC estimation accuracy. To overcome the shortcomings of the Ah-counting method, an enhanced CC method, called as modified CC is proposed in [5], where the losses are accounted as efficiency terms and the initial SoC is obtained based on any of the voltage methods; however, it is still an open-loop estimation method and has accumulated errors due to uncertainty in the initial SoC. In [6], both voltage method and CC method are combined for SoC estimation. This approach relies on the voltage method to avoid the error accumulation caused by the CC method. However, this approach is not suitable for shipboard applications where the disconnection of load may not be feasible. Online SoC estimation methods based on state observers like Kalman filter (KF), extended KF, adaptive KF, unscented KF, sigma-point KF, adaptive KF, dual KF, derivative KF, slide mode observer, and H∞ filter are also adopted for better accuracy [7]–[18]. In these works, KFs are used to determine the system's inner state which is the battery

Manuscript received July 10, 2020; revised September 29, 2020 and October 17, 2020; accepted October 22, 2020. Date of publication October 28, 2020; date of current version October 1, 2021. This work was supported by the Department of Science and Technology-Science and Engineering Research Board-(DST SERB), New Delhi, for the project "Optimal energy management system in shipboard microgrid with solar PV," under Grant TAR/2018/000412. Recommended for publication by Associate Editor Maryam Saeedifard. *(Corresponding author: Preetha Roselyn.)*

J. Preetha Roselyn is with the Department of EEE, SRM Institute of Science and Technology, Kattankulathur, India (e-mail: preethaj@srmist.edu.in).

Anirudhh Ravi is with NC State University, Raleigh, NC, USA (e-mail: aravi9@ncsu.edu).

D. Devaraj is with the Department of EEE, Kalasalingam Academy of Research and Education, Krishnankoil, India (e-mail: d.devaraj@klu.ac.in).

R. Venkatesan is with OOS, National Institute of Ocean Technology, Chennai, India (e-mail: venkat@niot.res.in).

Color versions of one or more figures in this article are available at https://doi.org/10.1109/JESTPE.2020.3034362.

Digital Object Identifier 10.1109/JESTPE.2020.3034362

SoC. This state estimation technique involves complexity in determining the initial parameter, relies on the need for an accurate and suitable battery model, and requires a large computation capacity makes the estimation strategy disadvantageous. Recently, intelligent techniques namely fuzzy logic and neural networks are adopted for enhancing the computation process and the accuracy in the estimation of SoC [19]–[27]. The risk of these intelligent techniques includes the accuracy of the methods being dependent on the sensitivity of the amount and quality of the training data. Additionally, it is uncertain whether those methods can work efficiently with batteries of different capacities and chemistries.

It is important to note that for an accurate SoC estimation, the effect of battery hysteresis on SoC estimation [28], [29] has to be accounted. Simple electric circuit-based models with ideal voltage source in series with an internal resistance do not account for the battery's SoC and the battery hysteresis effect [30], [31]. Alternatively, *RC* circuit models are proposed where there is an open voltage source with a series internal resistance and a shunt *RC* element known as Warburg impedance [32]. Additionally, different *RC* circuit-based battery models have been proposed [33]–[36]. The main disadvantage of this method is the difficulty in identifying the model parameters due to the use of impedance spectroscopy, which is a rather complex technique. Moreover, this model does not account for the battery hysteresis effect. A Warburg impedance-based dynamic model which models terminal voltage as a function of current and time was proposed in [37]. Though the model considers the nonlinear dependence of all circuit elements, first, the model relies on impedance spectroscopy to determine the model parameters, which is again difficult. Second, the model does not account for the relaxation term, which is important to be considered to model the hysteresis effect. In [38]and [39], a normalized battery model is developed by Copetti for PV applications in which voltage equations during the charge/discharge period are derived. The relation among the battery parameters and the behavior of internal resistance during the charge/discharge process is investigated. The electrochemical behavior of a battery has been modeled by Shepherd [40] considering the terminal and OCVs, SoC, internal resistance, and discharge current. The model accounts for the polarization phenomenon in the battery but cannot be implemented for this study since it has an inbuilt algebraic loop error. Hence, a modified Shepherd model [41] is widely adopted, where the polarization is modeled in terms of a polarization voltage term, rather than using a polarization resistance term.

This work uses a modified Shepherd model to construct a dynamic model of lead–acid batteries along with propeller load with chopper fed dc drive used in shipboard applications. Based on this characteristic, the hysteresis phenomenon is studied, and the proposed differential evolution (DE)-based SoC estimation technique is applied to accurately estimate SoC minimizing the hysteresis effect in conventional SoC estimation methods. The actual SoC is obtained from a battery after a long rest period. But in real-time, it is difficult to accommodate such long rest periods. Hence, this article provides a novel SoC estimation considering the hysteresis effect of the battery which minimizes the deviation in SoC

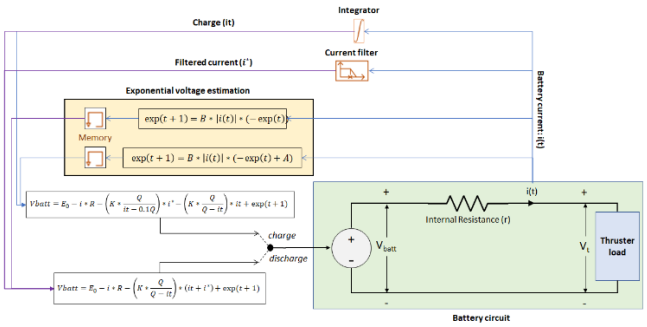

Fig. 1. Battery dynamic model for shipboard system.

estimation during charge and discharge strategies. An efficient BMS for charge and discharge control of the battery is also proposed that works based on the accurate SoC estimation by the proposed technique. The proposed system with accurate SoC tracking charges and discharges the battery efficiently and increases the battery lifetime, thereby, reducing the amount of capacity fade.

The main contributions of this work are as follows.

1) Development of a battery dynamic model for lead–acid batteries used in shipboard applications. This dynamic model includes exponential zone voltage term and models the relaxation voltage effect to accurately model the battery hysteresis.
2) An adaptive DE-based SoC estimation is proposed for accurate SoC estimation, where the hysteresis effect on SoC estimation is accounted for properly.
3) An efficient BMS algorithm is proposed for safe battery operation and extended battery life.
4) Validation of the proposed SoC estimation technique and BMS algorithm in a real-time marine Robo-boat.

II. Battery Dynamic Model for Shipboard System

In a shipboard system, thruster loads have the largest share in demand hence, a battery dynamic model with a thruster load is considered. In this work, discrete equations are used for charge and discharge cycles to accurately model the battery characteristics. The dynamic model of a battery used in a shipboard system is shown in Fig. 1.

A. Dynamic Discharge Model

This work uses a modified Shepherd model [40] to model the battery dynamics. Here, a polarization voltage term is added to the existing battery voltage equation to achieve precise tracking of battery voltage dynamics under varying battery discharge currents and a polarization resistance term is used to model the nonlinearity between the battery voltage and its SoC. The nominal battery discharge characteristics of a 12-V, 62-Ah lead-acid battery is shown in Fig. 2.

The exponential zone voltage term is given as

$$\dot{\exp}(t) = B * |i(t)| * (-\exp(t)) \tag{1}$$

where

$\dot{\exp}(t) =$ exponential zone voltage (V);
$i(t) =$ battery discharge current (A);
$B =$ exponential zone time constant inverse (Ah^{-1});

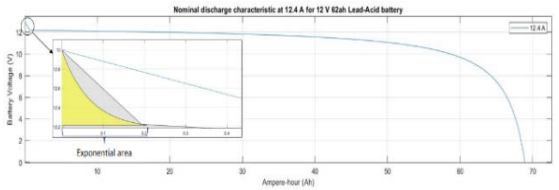

Fig. 2. Nominal battery discharge characteristic.

B. Dynamic Charge Model

As used in the dynamic discharge model, the dynamic charge model uses a modified Shepherd model. The dynamic charge model of the battery includes a polarization resistance term to account for the rapid rise in the battery voltage as the battery approaches full charge

$$\begin{aligned}&\text{Polarization resistance} = K\frac{Q_{\text{rated}}}{Q_{\text{actual}}}\\ &\text{At full charge, } Q_{\text{actual}} = \text{it} = 0\\ &\Rightarrow \text{Polarization resistance} = \infty. \end{aligned} \tag{2}$$

The above condition causes an algebraic loop error in simulation. This is overcome by incorporating a 10% shift from the actual battery capacity in the polarization resistance term. The resulting polarization resistance term during charging mode is given as

$$\text{Polarizationresistance} = K\frac{Q_{\text{rated}}}{Q_{\text{actual}} - (0.1 * Q_{\text{rated}})}. \tag{3}$$

Also, the exponential zone voltage term is expressed as

$$\dot{\exp}(t) = B * |i(t)| * (-exp(t) + A) \tag{4}$$

where A = exponential zone voltage amplitude

Accordingly, the battery voltage equation, V_{batt} during charge mode can be written as

$$\begin{aligned}V_{\text{batt}} = E_0 - (i(t) * R) - \left(K\frac{Q_{\text{rated}}}{Q_{\text{actual}} - (0.1 * \text{Q}_{\text{rated}})} i(t)^*\right)\\ - \left(K\frac{Q_{\text{rated}}}{Q_{\text{rated}} - Q_{\text{actual}}} Q_{\text{actual}}\right) + \dot{\exp}(t)\end{aligned} \tag{5}$$

where E_o is the internal emf and R is the internal resistance.

Batteries with chemicals like Pb–acid, nickel–metal–hydride, and nickel–cadmium have prominent hysteresis phenomenon which occurs in the exponential zone.

III. Proposed DE-Based SoC Estimation

A. Hysteresis Phenomenon and Its Effect on SoC Estimation

Hysteresis phenomenon in lead–acid batteries occurs due to an internal chemical conversion process and the time constant associated with that process. During the cell chemical conversion process, two processes, namely, charge transfer and mass transfer take place. Charge transfer refers to the chemical reaction that takes place at the electrode–electrolyte interface whose time constant is relatively very less compared to that of mass transfer where the transformed materials of the charge transfer process move away from the electrodes thereby giving space for new materials to be transformed. Due to these processes, there is a delay between the application of charging voltage and the actual chemical reaction to take place during charging and the connection of load and the supply of current from the battery during discharging. This phenomenon results in the hysteresis effect. For lead–acid batteries, this delay can be approximated in terms of time constants given as

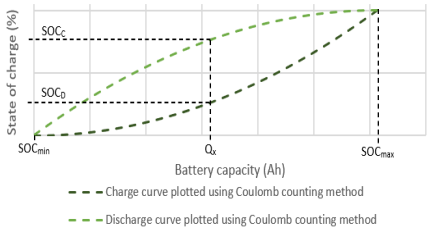

Fig. 3. Hysteresis plot of a lead–acid battery.

$$\tau_{\text{hys}} = \tau_1 + \tau_2 \tag{6}$$

where

τ_{hys} = net time constant associated with the delay causing hysteresis;

τ_1 = time constant associated with the charge transfer process;

τ_2 = time constant associated with the mass transfer process.

Due to the above-mentioned hysteresis phenomenon, there is a discrepancy in the estimation of the battery SoC. This is because, for any given battery capacity value (Q_x) that lies between SoC_{max} and SoC_{min}, there exists two SoC values, distinct for a charge cycle and a discharge cycle, as illustrated in Fig. 3. In CC-based SoC estimation [6], the following equations are used:

$$\text{During charging, } \text{SoC}_{\text{c}}(t) = \text{SoC}_c(t-1) + \frac{1}{C_{\text{rated}}}.\int i_c(t).dt \tag{7}$$

$$\text{During discharging, } \text{SoC}_{\text{d}}(t) = \text{SoC}_{\text{d}}(t-1) - \frac{1}{C_{\text{rated}}}.\int i_d(t).dt \tag{8}$$

where $\text{SoC}_c(t-1)$ and $\text{SoC}_d(t-1)$ are previous time SoC values, C_{rated} is the rated capacity, $i_c(t)$ and $i_d(t)$ are the charge and discharge currents.

The objective is to calculate the SoC hysteresis for a given battery capacity value. Let us consider a fixed point Q_x, for which $Q_x = Q_c = Q_d$, as shown in Fig. 3.

The value of SoC_{hys} corresponding to Q_x, can be obtained from (8) and (9) as follows:

$$\begin{aligned}\text{SoC}(t) - \text{SoC}_d(t) = \text{SoC}_c(t-1) - \text{SoC}_d(t-1)\\ + \frac{1}{C_{\text{rated}}}.\int i_c(t)dt + \frac{1}{C_{\text{rated}}}.\int i_d(t).dt\end{aligned} \tag{9}$$

This value of hysteresis for a given Q_x can be expressed mathematically as

$$\text{SoC}_{\text{hys}} = \frac{\text{SoC}_C - \text{SoC}_d}{\text{SoC}_{\text{max}} - \text{SoC}_{\text{min}}} \times 100\%. \tag{10}$$

For a complete charge and discharge cycle, the values of SoC_{max} and SoC_{min} are 100 and 0, respectively.

B. Problem Statement

In the CC-based SoC estimation, there is a huge difference between the estimated values of SoC during charging and the SoC during discharging for a given battery capacity, due to a large vertical distance between the charge and discharge curves

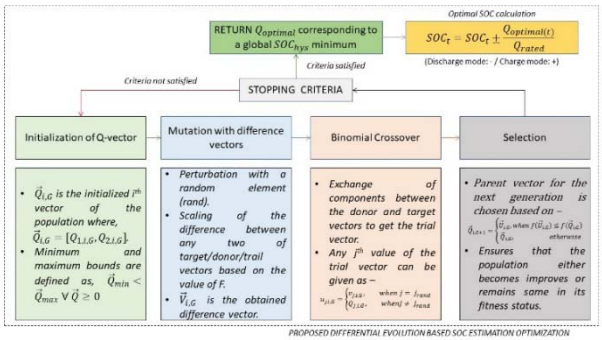

Fig. 4. Proposed adaptive DE-based SoC estimation.

at a given battery capacity point. This difference results in a huge hysteresis error that affects the accuracy of the SoC estimation. For the complete cycle, the $\mathrm{SoC_{hys}}$ given in (10) can be simplified as

$$\mathrm{SoC_{hys}} = (\mathrm{SoC}_C - \mathrm{SoC}_d) \times 100\%. \tag{11}$$

The proposed model achieves an optimal SoC value of the battery by minimizing the estimation error due to hysteresis as mentioned in (11). Hence, if a battery undergoes a complete charge and discharge cycle, the $\mathrm{SoC_{hys}}$ can be simply defined as the vertical distance between the charge and discharge curves of a battery SoC versus battery capacity plot.

C. Adaptive Differential Evolution for SoC Estimation

The working of the proposed adaptive DE-based SoC estimation for optimal SoC estimation is illustrated in Fig. 4. The following issues are addressed in the implementation of the proposed DE for SoC estimation:

1) Problem Representation: The initialized ith Q-parameter vector of the population corresponding to a Gth generation is represented as

$$\vec{Q}_{i,G} = [Q_{1,i,G}, Q_{2,i,G}]. \tag{12}$$

Since the value of Q should always be positive, a range is defined such that the search space lies in the positive coordinate.

This range can be defined as

$$\vec{Q}_{\min} \leq \vec{Q} \leq \vec{Q}_{\max} \quad \forall \vec{Q} \geq 0. \tag{13}$$

Therefore, any jth component of an ith Q-vector at a given generation can be represented as

$$Q_{j,i,0} = Q_{j,\min} + \mathrm{rand}_{i,j}[0, 1]\left(Q_{j,\max} - Q_{j,\min}\right). \tag{14}$$

2) Evaluation Function: In the proposed optimized SoC estimation, the objective function is minimization of $\mathrm{SoC_{hys}}$ which is the vertical distance between the charge and discharge curves for a particular battery capacity. This minimization problem leads to accurate SoC estimation as the proposed problem minimizes the hysteresis estimation error in the charge and discharge cycle of the battery. The inequality constraint is the Q parameter provided in (16). The constraint is considered by adding a quadratic penalty function to the objective function. With the inclusion of the penalty function, the new objective function becomes

$$\mathrm{Min}\, f = \mathrm{SoC_{hys}} + QP \tag{15}$$

where QP is the penalty term for Q parameter

$$\mathrm{QP} = \begin{Bmatrix} k_p\left(Q_j - Q_{j\max}\right)^2 \text{ if } Q_j > Q_{j\max} \\ k_p\left(Q_j - Q_{j\min}\right)^2 \text{ if } Q_j < Q_{j\min} \\ 0 \quad \text{otherwise} \end{Bmatrix} \tag{16}$$

where k_p is the penalty factor which is obtained using the correct combination in the problem. Since DE maximizes the fitness function, the minimization objective function f is transformed to a fitness function to be maximized as

Fitness $= k/f$, where k is a large constant.

Compared to other evolutionary algorithms, the main advantage of DE is that it is a stochastic real-parameter optimization algorithm. The DE algorithm starts with the initialization of parameter (battery capacity) vectors and searches for a global optimum point in the 2-D space.

In this work, DE/RandSF/1/bin strategy scheme with a self-tuned parameter which employs binomial crossover and difference vector-based mutation is employed. RandSF denotes a random scale vector to be perturbed, 1 denotes the number of difference vectors considered for perturbation and bin stands for binomial crossover operator. Since the control parameters like mutation scale factor (F), crossover constant (C_r), and population size (NP) have an individual effect on the DE performance, it is necessary to carefully choose the values of these parameters. From the literature survey, it was known that for a 2-D problem, since the function parameters (Q, $\mathrm{SoC_{hys}}$) are dependent, the optimal value of C_r is chosen from the range of [0.7, 1]. The scale factor, F is varied randomly in the range of [0.4, 0.95] by using the relation

$$F = 0.4 \times [1 + \mathrm{rand}(0, 1)] \tag{17}$$

where rand (0,1) is the uniformly distributed random number within the range (0,1). This allows for the stochastic variations in the amplification of the difference vector and thus helps retain population diversity as the search progresses.

IV. Battery Management System in Shipboard Battery

An effective BMS not only results in efficient battery operation but also enhances the battery lifetime. The proposed BMS controls the battery charging and discharging process based on the battery SoC levels. This BMS algorithm relies on accurate SoC estimation based on the adaptive DE (ADE) algorithm. To describe the working of the proposed system, the system is categorized into four zones: estimation zone, charge zone, discharge zone, and charge/discharge control zone as shown in Fig. 5. To start with, in the charge and discharge zones, the battery is connected to a battery charger and a thruster load, respectively, for the battery to charge and discharge. Next, in the estimation zone, the parameters required by the BMS algorithm are estimated. In this zone, the estimation system starts by estimating the battery SoC based on an initial SoC value. Subsequently, this initial SoC value is fed to the adaptive DE algorithm and the battery SoC value is estimated accurately. Furthermore, the SoH estimation takes place based on the estimated battery SoC. Initially, in the first iteration, the battery SoH is obtained based on the formula indicated in Fig. 5. In subsequent iterations, the battery SoH

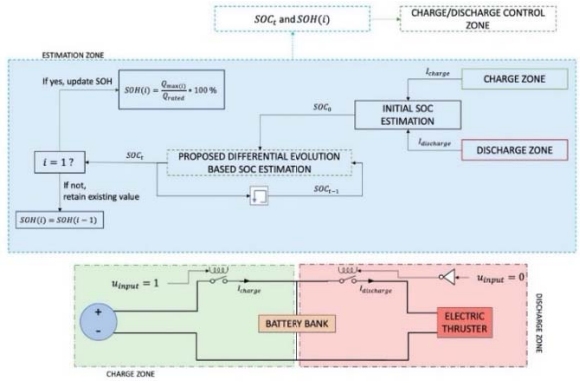

Fig. 5. Proposed BMS with adaptive DE-based SoC estimation.

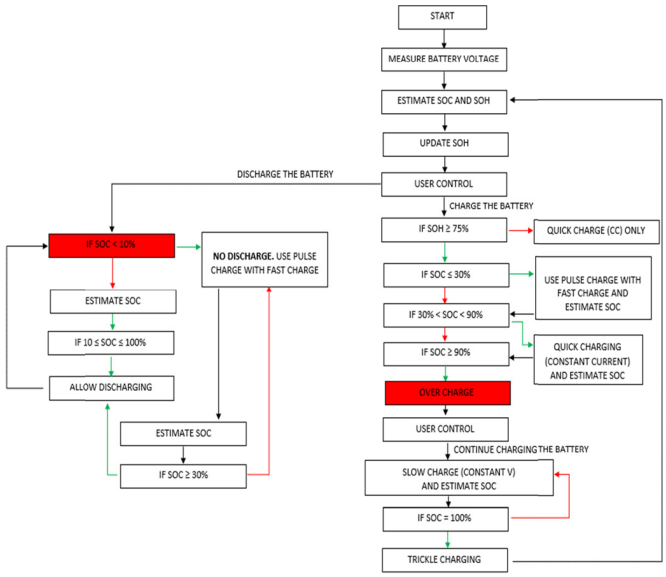

Fig. 6. Proposed BMS based on the estimated SoC.

is maintained at a value equal to that in the previous iteration. The calculated values of SoC and SoH are fed to the proposed BMS algorithm in the charge/discharge control zone. The working of the system zones is explained in more detail as follows:

The optimization achieved through DE enables accurate tracking of SoC essential for the effective working of the proposed BMS algorithm as depicted in Fig. 6. The proposed algorithm compares the battery SoC with specific limits and commands the battery charging or discharging process. In addition to the battery SoC, consideration of its SoH is also crucial since practicing fast charging methods or deep cycling to a battery which is already deteriorating only makes the battery's condition worse. Hence, in charging mode, the proposed algorithm not only considers the battery SoC but also its SoH to achieve safe charging for a longer lifetime, an added advantage, whereas, in discharging mode, the algorithm by default switches from discharging to charging mode if the SoC is less than 10%. The algorithm also includes a user interactive feature, where, the user can choose between charging and discharging modes.

The different charging methods based on the SoC level are provided in Table I. If the battery SoC is less than 30%, the battery is considered to be almost dead hence, voltage pulse charging is used to revive the battery. This method uses high-frequency voltage pulses of amplitude greater than the nominal voltage of the battery. Next, if the battery SoC lies in the range of 30%–90%, quick charging is adopted. Here, the charging voltage is maintained at a value equal to the rated OCV of the battery and the charge supplied to the battery is 0.1 times the rated capacity. If the battery SoC is greater than 90% but not equal to 100%, the charging voltage is maintained at the same value as that during quick charging, but the charge supplied to the battery is 0.01 times the rated capacity. Finally, if the battery SoC is exactly 100%, then trickle charging is adopted where the charging voltage is maintained at the nominal voltage of the battery so that there is no potential difference between the charger and battery.

TABLE I
CHARGING METHODS BASED ON THE BATTERY SOC

SoC level	Charging method
[0%, 30%]	Pulse Charging
[30%, 90%]	Quick Charging
[90%, 100%]	Trickle Charging

Since deep cycling of the battery results in a gradual deterioration of battery lifetime, the proposed algorithm ensures that the operating range of the battery SoC is maintained between 30% and 100%. But, if due to some emergency the battery has been discharged below 30% of SoC, then the proposed algorithm fast charges the battery until the battery SoC reaches 30%.

V. RESULTS AND DISCUSSION

A. Simulation Results

A 12-V, 100-Ah valve-regulated lead–acid battery is simulated using a dynamic model in MATLAB/Simulink 2018a. A thruster load of 5 HP is connected to the battery via a four-quadrant dc/dc chopper. The operating conditions of the 100-Ah battery are—SoC: 0%–100%, battery capacity: 0–100 Ah, tested discharge currents: 1, 10, 50, 100, 150, and 200 A, number of cycles: 680 cycles, battery voltage: 0–12 V. One complete cycle of charge and discharge is conducted to capture the entire range of remaining battery capacity variation for the change in the SoC. To validate the performance of the proposed BMS in the shipboard system, the proposed charging method is applied for a simulation time of about 1 year. This is then compared with a battery model, without the proposed BMS after a period of 680 cycles of charge and discharge. It is shown that there is a difference of 3.77 Ah in the maximum capacity of the battery when the proposed BMS algorithm is implemented. Correspondingly, the state of health is also increased by 3.77% with the inclusion of the BMS algorithm. It can be inferred from Table II that the charging algorithm preserves the life expectancy of the battery and its maximum capacity. Hence, the proposed charging algorithm is efficient in maintaining the overall health of the battery.

To achieve the objective of reducing the SoC estimation error for an efficient BMS, a single objective function-based DE algorithm is applied. The DE search space is limited within the range $\vec{Q} \in [0,100]$ Ah. The estimated battery SoC versus battery capacity using the proposed DE-based SoC estimation

TABLE II

PERFORMANCE OF BATTERY USING THE PROPOSED BMS CHARGING ALGORITHM

Algorithm Implemented	Maximum capacity after 680 cycles	State of health after 680 cycles
Without BMS	49.83 Ah	49.83%
With BMS	53.6 Ah	53.6 %

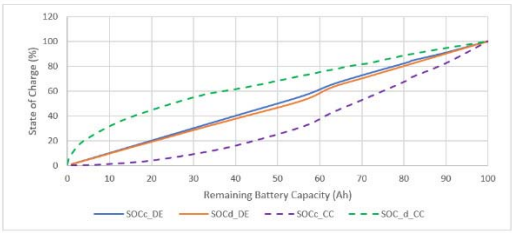

Fig. 7. SoC versus remaining battery capacity using DE-based SoC estimation for full charge/discharge cycle.

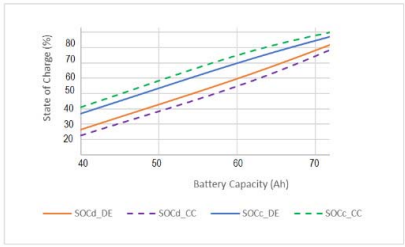

Fig. 8. SoC versus remaining battery capacity using DE-based SoC estimation for partial charge/discharge cycle.

TABLE III

COMPARISON OF PERFORMANCE OF CC METHOD AND PROPOSED DE METHOD

Capacity (Ah)	SoC charge (CC)	SoC charge (DE)	Error Charge (%)	SoC discharge (CC)	SoC discharge (DE)	Error discharge (in %)
1	4.62	1	-3.62	0.01	0.98	+0.97
41.5	46.82	41.5	-5.32	17.21	38.98	+21.77
84.46	80.73	84.46	-3.73	71.22	82	+10.78
90.82	87.24	90.82	-3.58	82.33	90	+7.67

method is compared with the CC method and is plotted in Figs. 7 and 8 for full and partial charge/discharge cycles which resembles a closed hysteresis loop for the full cycle. It is seen that the CC method overestimates the SoC of the battery, as it accounts for increased SoC hysteresis as shown in Table III. On the other hand, the DE model accurately estimates the SoC of the battery, due to the reduction of the SoC hysteresis error. On average, the DE model estimates the SoC closer to the true value since the DE model reduces the error in SoC estimation due to hysteresis (SoC_{hys}), as summarized in Table IV. On an average, the SoC_{hys} accounted for in the CC method is 14.147% while it is reduced to 1.2706% in the proposed method as shown in Fig. 9. As the proposed method reduces the hysteresis in measurement, it estimates both charging and discharging SoC more accurately than the CC method.

The estimated capacity and SoC from the DE model at the charging and discharging cycle is used and plotted against the voltage of the battery obtained during charge and discharge. It can be observed from the battery voltage versus battery

TABLE IV

COMPARISON OF HYSTERESIS ERROR IN SOC MEASUREMENT

Q (Ah)	SoC_{hys} (CC)	SoC_{hys} (DE)	SoC_{err} (%)
1	4.61	0.02	4.59
6	7.71	0.33	7.38
32	21.31	1.69	19.62
41.5	29.61	2.52	27.09
56	40.81	3.64	37.17
84.46	9.51	2.46	7.05
90.82	4.91	0.82	4.09
100	4.41	0	4.41

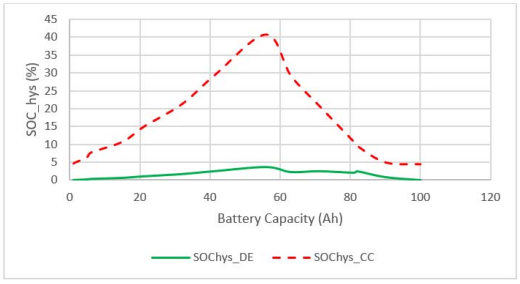

Fig. 9. SoC_{hys} versus battery capacity using proposed DE and CC method.

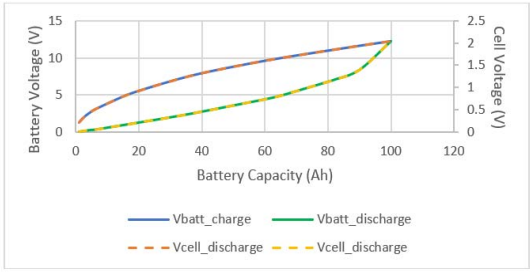

Fig. 10. Voltage versus battery capacity using the proposed DE model.

capacity graph as shown in Fig. 10 that there is a presence of battery hysteresis. This presence is observed due to the exponential zone voltage term accounted for in the battery dynamic model. The dynamic test is conducted on the battery model along with the proposed algorithm under varying thruster load conditions and is provided in Fig. 11.

The heat dissipation under varying discharge currents along with SoC estimation is provided in Fig. 12. A curve fitting method for the proposed model is implemented and is shown in Fig. 13. The fitted regression equation has a determination coefficient of 0.9999 for the charging condition while it is 0.9997 for the discharging condition. Hence, the generated equations are valid and can be used for accurate modeling and studying the characteristics of a 100-Ah lead acid battery based on the proposed SoC estimation method.

B. Experimental Results

The proposed DE-based battery SoC estimation is evaluated in a shipboard system with a thruster load. The schematic, hardware setup, and front-end monitoring platform after the implementation of the proposed BMS are provided in Figs. 14–16, respectively. A 12-V, 62-Ah secondary lead–acid battery is used to supply power to a boat thruster load of 25 HP. The operating conditions of the 62-Ah battery are—SoC:

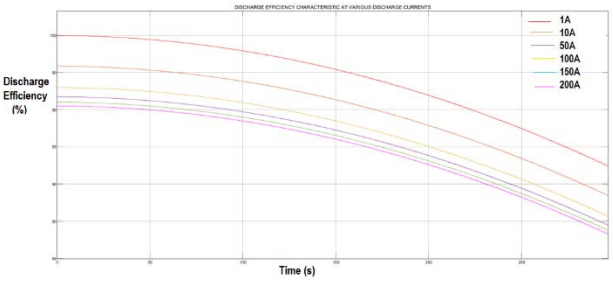

Fig. 11. Discharge efficiency under varying discharge currents.

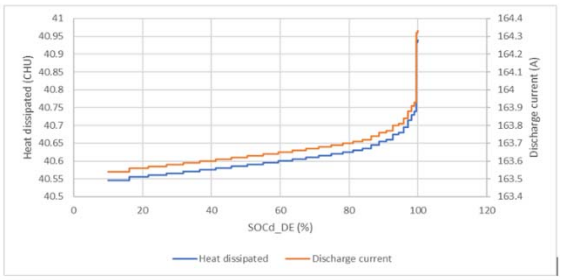

Fig. 12. Heat dissipation and SoC under varying discharge currents.

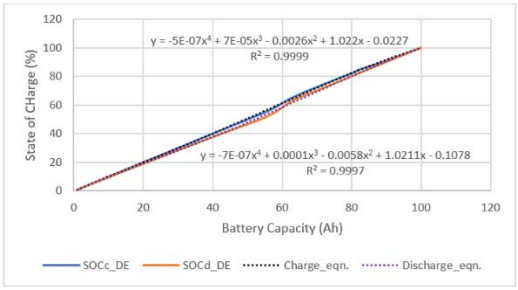

Fig. 13. SoC curve fit equation versus battery capacity for 100-Ah battery.

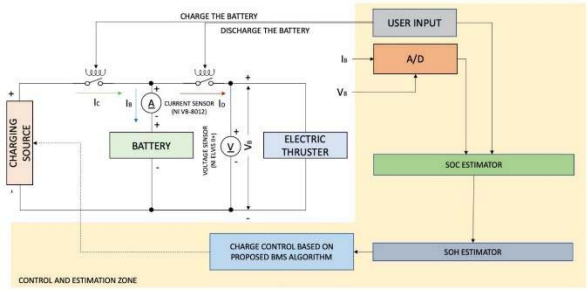

Fig. 14. Schematic of thruster load hardware setup.

0%–100%, battery capacity: 0 to 62 Ah, tested discharge currents: 5 and 10 A, and battery voltage: 0–12 V. The charging and discharging of the battery are provided through a bidirectional buck-boost converter of 1.5 kW. The proposed SoC estimation is programmed in a SPARTAN6 FPGA board. The LabVIEW software works as a front-end display for monitoring the battery parameters which is connected to the FPGA board using a serial port communication.

The DE search space is limited within the range $\vec{Q} \in [0, 62]$ Ah. The SoC versus battery capacity obtained using the proposed model is compared with the CC method and is plotted in Fig. 17. This results in a more accurate SoC

Fig. 15. Hardware setup with thruster load.

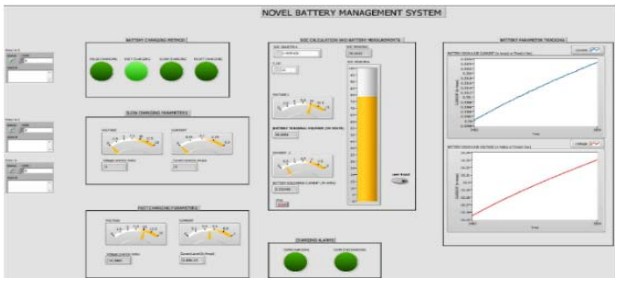

Fig. 16. Real-time monitoring of BMS.

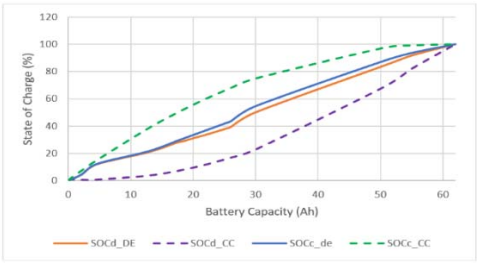

Fig. 17. SoC versus battery capacity using DE model and CC method.

TABLE V
COMPARISON OF PERFORMANCE OF CC METHOD AND PROPOSED METHOD

Capacity (Ah)	SoC_{charge} (CC)	SoC_{charge} (DE)	$Error_{charge}$ (%)	$SoC_{discharge}$ (CC)	$SoC_{discharge}$ (DE)	$Error_{discharge}$ (%)
2.1684	7.2976	4.4713	2.8263	0.5752	4.3847	-3.8095
4.6373	15.0202	12.2001	2.8201	0.6713	11.9589	-11.2876
12.8622	38.3198	21.44	16.8798	3.6124	20.77	-17.1576
18.3938	51.8896	30.6647	21.2249	7.858	28.7968	-20.9388
20.4502	56.5036	34.092	22.4116	9.9014	31.5424	-21.641
22.2942	60.4424	37.1653	23.2771	11.948	33.8726	-21.9246
30	74.8714	54.517	20.3537	22.6935	49.9999	-27.3064
62	100	100	0	100	100	0

estimation as the proposed model reduces the SoC estimation error and does not eliminate the phenomenon of hysteresis, rather accounting for it more accurately.

The proposed SoC estimation method estimates the battery SoC closer to the true value which can be observed from Table V. The reduction in the estimated SoC value, when compared with the CC method, in charging mode and an increase in the estimated SoC value, when compared with the CC method, in discharging mode are depicted in Fig. 18.

TABLE VI
COMPARISON OF HYSTERESIS ERROR IN SOC MEASUREMENT

Q (Ah)	SoC_{hys} (CC)	SoC_{hys} (DE)
4.6373	3.89×10^{-3}	0.2314339
18.3938	3.01×10^{-2}	0.7101871
25.52561	6.68×10^{-2}	0.8204694
50.4319	5.67×10^{-2}	0.4668548
62	0	0

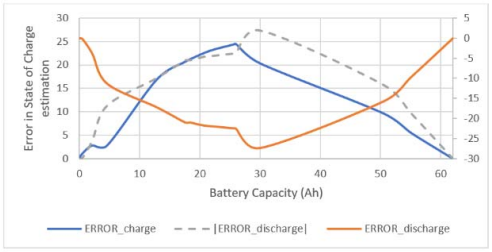

Fig. 18. SoC error versus battery capacity in SoC estimation using CC method.

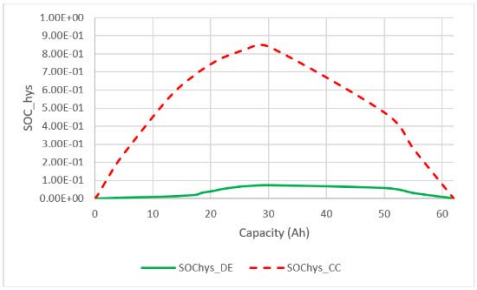

Fig. 19. SoC_{hys} versus battery capacity using DE and CC method.

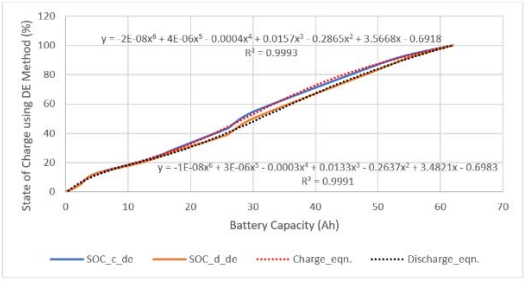

Fig. 20. SoC curve fit equation versus battery capacity for 62-Ah battery.

From Table VI, it can be noted that the proposed SoC estimation strategy reduces the average SoC estimation hysteresis by 40.79% from 0.47 to 0.00303 for the 62-Ah battery. From this observation, it can be inferred that the proposed estimation strategy reduces the deviation of the estimated SoC values under charging and discharging cycles from the true value and does not eliminate the hysteresis phenomenon as shown in Fig. 19.

Using the battery capacity and SoC data obtained in charging and discharging process, a curve fitting was done to obtain a mathematical relationship between the estimated SoC by the DE method and the battery capacity. From Fig. 20, it can be seen that the curve fit equations have a coefficient of determination (R^2) value close to 1 which implies that these equations map the estimated SoC value.

VI. CONCLUSION

This work started with the study of the necessity for an accurate battery SoC estimation for an enhanced performance of a BMS. It has been observed from the study that battery hysteresis plays a crucial role in the performance of an SoC estimation technique. Hence, in this work, an enhanced optimization technique like DE was adopted whose objective was to reduce the vertical distance between the two estimated SoC values, during charge and discharge cycles, for a given battery capacity. Based on the results obtained, it has been observed that the proposed DE-based battery SoC technique achieves the objective and accounts for the battery hysteresis phenomenon more accurately. For easy applicability of the technique in a real-time battery SoC estimation system, the proposed work provides a direct mathematical relationship between the battery capacity and the estimated SoC for batteries with capacities generally adopted in a marine application, such as 100 and 62 Ah.

ACKNOWLEDGMENT

The authors thank the MOES, SRMIST, and KARE for all the support and facilities extended and the Director, NIOT, for all his continuous support.

REFERENCES

[1] R. Xiong, J. Cao, Q. Yu, H. He, and F. Sun, "Critical review on the battery state of charge estimation methods for electric vehicles," *IEEE Access*, vol. 6, pp. 1832–1843, 2018.
[2] W.-Y. Chang, "The state of charge estimating methods for battery: A review," *ISRN Appl. Math.*, vol. 2013, no. 1, pp. 1–7, 2013.
[3] S. Sato and A. Kawamura, "A new estimation method of state of charge using terminal voltage and internal resistance for lead acid battery," in *Proc. Power Convers. Conf.-Osaka*, Apr. 2002, vol. 2, no. 3, pp. 565–570, 2002.
[4] M. Murnane and A. Ghazel, "A closer look at State of Charge (SOC) and State of Health (SOH) estimation techniques for batteries," Analog Devices, Norwood, MA, USA, Tech. Rep., 2017, pp. 1–8. [Online]. Available: http://www.analog.com
[5] K. S. Ng, C.-S. Moo, Y.-P. Chen, and Y.-C. Hsieh, "Enhanced Coulomb counting method for estimating state-of-charge and state-of-health of lithium-ion batteries," *Appl. Energy*, vol. 86, no. 9, pp. 1506–1511, Sep. 2009.
[6] M. Verbrugge and E. Tate, "Adaptive state of charge algorithm for nickel metal hydride batteries including hysteresis phenomena," *J. Power Sources*, vol. 126, nos. 1–2, pp. 236–249, 2004.
[7] M. Ye, H. Guo, and B. Cao, "A model-based adaptive state of charge estimator for a lithium-ion battery using an improved adaptive particle filter," *Appl. Energy*, vol. 190, pp. 740–748, Mar. 2017.
[8] J. Li, J. Klee Barillas, C. Guenther, and M. A. Danzer, "A comparative study of state of charge estimation algorithms for LiFePO4 batteries used in electric vehicles," *J. Power Sources*, vol. 230, pp. 244–250, May 2013.
[9] S. Sepasi, R. Ghorbani, and B. Y. Liaw, "A novel on-board state-of-charge estimation method for aged li-ion batteries based on model adaptive extended Kalman filter," *J. Power Sources*, vol. 245, pp. 337–344, Jan. 2014.
[10] I.-S. Kim, "A technique for estimating the state of health of lithium batteries through a dual-sliding-mode observer," *IEEE Trans. Power Electron.*, vol. 25, no. 4, pp. 1013–1022, Apr. 2010.
[11] F. Sun, X. Hu, Y. Zou, and S. Li, "Adaptive unscented Kalman filtering for state of charge estimation of a lithium-ion battery for electric vehicles," *Energy*, vol. 36, no. 5, pp. 3531–3540, May 2011.
[12] C. Zou, C. Manzie, D. Nešić, and A. G. Kallapur, "Multi-time-scale observer design for state-of-charge and state-of-health of a lithium-ion battery," *J. Power Sources*, vol. 335, pp. 121–130, Dec. 2016.
[13] Y. Wang, C. Zhang, and Z. Chen, "On-line battery state-of-charge estimation based on an integrated estimator," *Appl. Energy*, vol. 185, pp. 2026–2032, Jan. 2017.
[14] D. E. Acuña and M. E. Orchard, "Particle-filtering-based failure prognosis via sigma-points: Application to lithium-ion battery state-of-charge monitoring," *Mech. Syst. Signal Process.*, vol. 85, pp. 827–848, Feb. 2017.

[15] Z. Wei, R. Xiong, T. M. Lim, S. Meng, and M. Skyllas-Kazacos, "Online monitoring of state of charge and capacity loss for vanadium redox flow battery based on autoregressive exogenous modeling," *J. Power Sources*, vol. 402, pp. 252–262, Oct. 2018.
[16] Y. Zhang, C. Zhao, and S. Zhu, "State-of-charge estimation of li-ion batteries based on a hybrid model using nonlinear autoregressive exogenous neural networks," in *Proc. IEEE PES Asia–Pacific Power Energy Eng. Conf. (APPEEC)*, Oct. 2018, pp. 772–777.
[17] W. He, N. Williard, C. Chen, and M. Pecht, "State of charge estimation for li-ion batteries using neural network modeling and unscented Kalman filter-based error cancellation," *Int. J. Electr. Power Energy Syst.*, vol. 62, pp. 783–791, Nov. 2014.
[18] R. Zhang *et al.*, "State of the art of lithium-ion battery SOC estimation for electrical vehicles," *Energies*, vol. 11, no. 7, p. 1820, Jul. 2018.
[19] I.-H. Li, W.-Y. Wang, S.-F. Su, and Y.-S. Lee, "A merged fuzzy neural network and its applications in battery state-of-charge estimation," *IEEE Trans. Energy Convers.*, vol. 22, no. 3, pp. 697–708, Sep. 2007.
[20] P. Singh, R. Vinjamuri, X. Wang, and D. Reisner, "Design and implementation of a fuzzy logic-based state-of-charge meter for li-ion batteries used in portable defibrillators," *J. Power Sources*, vol. 162, no. 2, pp. 829–836, Nov. 2006.
[21] A. J. Salkind, C. Fennie, P. Singh, T. Atwater, and D. E. Reisner, "Determination of state-of-charge and state-of-health of batteries by fuzzy logic methodology," *J. Power Sources*, vol. 80, nos. 1–2, pp. 293–300, Jul. 1999.
[22] T. Parthiban, R. Ravi, and N. Kalaiselvi, "Exploration of artificial neural network [ANN] to predict the electrochemical characteristics of lithium-ion cells," *Electrochim. Acta*, vol. 53, no. 4, pp. 1877–1882, 2007.
[23] P. Singh, C. Fennie, and D. Reisner, "Fuzzy logic modelling of state-of-charge and available capacity of nickel/metal hydride batteries," *J. Power Sources*, vol. 136, no. 2, pp. 322–333, 2004.
[24] Y. S. Lee, W. Y. Wang, and T. Y. Kuo, "Soft computing for battery state-of-charge (BSOC) estimation in battery string systems," *IEEE Trans. Ind. Electron.*, vol. 55, no. 1, pp. 229–239, Jan. 2008.
[25] E. Chemali, P. J. Kollmeyer, M. Preindl, and A. Emadi, "State-of-charge estimation of li-ion batteries using deep neural networks: A machine learning approach," *J. Power Sources*, vol. 400, pp. 242–255, Oct. 2018.
[26] Y. Che, Y. Liu, Z. Chang, and J. Zhang, "SOC and SOH identification method of li-ion battery based on SWPSO-DRNN," *IEEE J. Emerg. Sel. Topics Power Electron.*, early access, Jun. 25, 2020, doi: 10.1109/JESTPE.2020.3004972.
[27] C. Burgos, D. Saez, M. E. Orchard, and R. Cardenas, "Fuzzy modelling for the state-of-charge estimation of lead-acid batteries," *J. Power Sources*, vol. 274, pp. 355–366, 2015.
[28] M. García-Plaza, J. Eloy-García Carrasco, A. Peña-Asensio, J. Alonso-Martínez, and S. Arnaltes Gómez, "Hysteresis effect influence on electrochemical battery modeling," *Electr. Power Syst. Res.*, vol. 152, pp. 27–35, Nov. 2017.
[29] M. A. Roscher, O. Bohlen, and J. Vetter, "OCV hysteresis in li-ion batteries including two-phase transition materials," *Int. J. Electrochem.*, vol. 2011, pp. 1–6, 2011.
[30] J. Kowal, D. Schulte, D. U. Sauer, and E. Karden, "Simulation of the current distribution in lead-acid batteries to investigate the dynamic charge acceptance in flooded SLI batteries," *J. Power Sources*, vol. 191, no. 1, pp. 42–50, Jun. 2009.
[31] M. Dürr, A. Cruden, S. Gair, and J. R. McDonald, "Dynamic model of a lead acid battery for use in a domestic fuel cell system," *J. Power Sources*, vol. 161, no. 2, pp. 1400–1411, 2006.
[32] E. Kuhn, C. Forgez, P. Lagonotte, and G. Friedrich, "Modelling ni-mH battery using cauer and foster structures," *J. Power Sources*, vol. 158, no. 2, pp. 1490–1497, Aug. 2006.
[33] M. Chen and G. A. Rincón-Mora, "Accurate electrical battery model capable of predicting runtime and I-V performance," *IEEE Trans. Energy Convers.*, vol. 21, no. 2, pp. 504–511, Jun. 2006.
[34] M. A. Roscher, J. Vetter, and D. U. Sauer, "Characterisation of charge and discharge behaviour of lithium ion batteries with olivine based cathode active material," *J. Power Sources*, vol. 191, no. 2, pp. 582–590, 2009.
[35] S. Buller, M. Thele, R. W. A. A. Dedoncker, and E. Karden, "Impedance-based simulation models of supercapacitors and li-ion batteries for power electronic applications," *IEEE Trans. Ind. Appl.*, vol. 41, no. 3, pp. 742–747, May 2005.
[36] E. Barsoukov, J. H. Kim, C. O. Yoon, and H. Lee, "Universal battery parameterization to yield a non-linear equivalent circuit valid for battery simulation at arbitrary load," *J. Power Sources*, vol. 83, nos. 1–2, pp. 61–70, Oct. 1999.
[37] P. Mauracher and E. Karden, "Dynamic modelling of lead/acid batteries using impedance spectroscopy for parameter identification," *J. Power Sources*, vol. 67, nos. 1–2, pp. 69–84, Jul. 1997.
[38] J. B. Copetti, E. Lorenzo, and F. Chenlo, "A general battery model for PV system simulation," *Prog. Photovolt., Res. Appl.*, vol. 1, no. 4, pp. 283–292, 1993.
[39] J. B. Copetti and F. Chenlo, "Lead/acid batteries for photovoltaic applications. Test results and modeling," *J. Power Sources*, 47, pp. 109–118, Jan. 1994.
[40] C. M. Shepherd, "Design of primary and secondary cells: II. An equation describing battery discharge," *J. Electrochem. Soc.*, vol. 112, no. 7, pp. 657–664, 1965.
[41] O. Tremblay, L.-A. Dessaint, and A.-I. Dekkiche, "A generic battery model for the dynamic simulation of hybrid electric vehicles," in *Proc. IEEE Vehicle Power Propuls. Conf.*, Sep. 2007, pp. 284–289.

J. Preetha Roselyn (Member, IEEE) received the M.S. degree from Anna University, in 2007, and the Ph.D. degree from SRMIST, Chennai, India, in 2015.

She is working as an Associate professor with the Department of EEE, SRMIST. She has received DST funded project in the topic "optimal energy management system in shipboard power system with solar PV." She has authored 34 journal and 35 conference publications and one book, and holds one patent. Her areas of specialization are voltage stability, computational intelligent techniques, grid integration issues of renewable energy, and building automation.

Anirudhh Ravi (Member, IEEE) is currently pursuing the master's degree in electric power systems engineering with NC State University, Raleigh, NC, USA.

His areas of research expertise include microgrid control and protection, battery energy storage systems, energy and battery management systems, and grid integration issues of renewable energy.

D. Devaraj (Senior Member, IEEE) received the Ph.D. degree from IIT Madras, Chennai, India, in 2001.

He is currently the Dean with the School of Electronics and Electrical Technology, Kalasalingam Academy of Research and Academy (KARE), Krishnankoil, India. He has authored two text books, power system analysis, and power system control, and 150 journal and 250 conference publications, and coauthored three text books. He has undertaken three research projects sponsored by DST, Government of India. His research interests include power system optimization, power system security, renewable energy, and smart grid.

Dr. Devaraj is the Secretary of IEEE Madras Section and Vice-Chair (Educational Activities) of IEEE India Council.

R. Venkatesan (Senior Member, IEEE) received the Ph.D. degree from the Indian Institute of Science, Bangalore, India, in 2001.

He is currently the Head of the Ocean Observation Group, National Institute of Ocean Technology, Chennai, India. He is also the Vice Chairman-Asia of the Data Buoy Cooperation Panel and the Chair of the International Tsunameter Partnership.

Dr. Venkatesan was a recipient of the Certificate of Merit by the World Meteorological Organization and UNESCO IOC for his outstanding services in global ocean data collection and the prestigious MTS Lockheed Martin Award and the National Geoscience Award from the Honorable President of India, and the MTS Fellow Award at IEEE/MTS Oceans Seattle. He is serving as a member of EXECOM of the IEEE Madras Section, served as the Chairman of IEEE OES India section, and has been reviewing articles for IEEE/MTS Oceans Conferences and is actively working to promote ocean engineering among the students. He is also teaching in Indian Premier Institutions IITs and was a Fulbright Scholar.